ISSN 1674-1056
http://cpb.iphy.ac.cn
http://iopscience.iop.org/cpb
中国物理 B
Chinese Physics
中国物理
Chinese Physics B

Numerical study on permeability characteristics of fractal porous media

Yongping Huang(黄永平), Feng Yao(姚峰), Bo Zhou(周博), Chengbin Zhang(张程宾)
Citation: Chin. Phys. B . 2020, 29(5): 054701 . **doi:** 10.1088/1674-1056/ab7b53
Journal homepage: http://cpb.iphy.ac.cn; http://iopscience.iop.org/cpb

What follows is a list of articles you may be interested in

Experimental study and theoretical analysis of fluid resistance in porous media of glass spheres

Tong Wang(王彤), Kun-Can Zheng(郑坤灿), Yu-Peng Jia(贾宇鹏), Cheng-Lu Fu(付承鹭), Zhi-Jun Gong(龚志军), Wen-Fei Wu(武文斐)
Chin. Phys. B . 2017, 26(7): 074701 . **doi:** 10.1088/1674-1056/26/7/074701

Dual solutions in boundary layer flow of Maxwell fluid over a porous shrinking sheet

Krishnendu Bhattacharyya, Tasawar Hayat, Ahmed Alsaedi
Chin. Phys. B . 2014, 23(12): 124701 . **doi:** 10.1088/1674-1056/23/12/124701

Bifurcation phenomena and control for magnetohydrodynamic flows in a smooth expanded channel

G. C. Layek, Mani Shankar Mandal, H. A. Khalaf
Chin. Phys. B . 2014, 23(11): 114701 . **doi:** 10.1088/1674-1056/23/11/114701

A fractal approach to low velocity non-Darcy flow in a low permeability porous medium

Cai Jian-Chao
Chin. Phys. B . 2014, 23(4): 044701 . **doi:** 10.1088/1674-1056/23/4/044701

Cross-diffusive effects on the onset of the double-diffusive convection in a horizontal saturated porous fluid layer heated and salted from above

Rajib Basu, G. C. Layek
Chin. Phys. B . 2013, 22(5): 054702 . **doi:** 10.1088/1674-1056/22/5/054702

Numerical study on permeability characteristics of fractal porous media*

Yongping Huang(黄永平)[1], Feng Yao(姚峰)[2], Bo Zhou(周博)[2], and Chengbin Zhang(张程宾)[1,†]

[1] *Key Laboratory of Energy Thermal Conversion and Control of Ministry of Education, School of Energy and Environment, Southeast University, Nanjing* 210096, *China*

[2] *Jiangsu Key Laboratory of Micro and Nano Heat Fluid Flow Technology and Energy Application, School of Environmental Science and Engineering, Suzhou University of Science and Technology, Suzhou* 215009, *China*

(Received 19 December 2019; revised manuscript received 19 January 2020; accepted manuscript online 1 March 2020)

The fractal Brownian motion is utilized to describe pore structures in porous media. A numerical model of laminar flow in porous media is developed, and the flow characteristics are comprehensively analyzed and compared with those of homogeneous porous media. Moreover, the roles of the fractal dimension and porosity in permeability are quantitatively described. The results indicate that the pore structures of porous media significantly affect their seepage behaviors. The distributions of pressure and velocity in fractal porous media are both non-uniform; the streamline is no longer straight but tortuous. When Reynolds number $Re < 1$, the dimensionless permeability is independent of Reynolds number, but its further increase will lead to a smaller permeability. Moreover, due to the higher connectivity and enlarged equivalent aperture of internal channel network, the augment in porosity leads to the permeability enhancement, while it is small and insensitive to porosity variation when $\varepsilon < 0.6$. Fractal dimension also plays a significant role in the permeability of porous media. The increase in fractal dimension leads to the enhancement in pore connectivity and a decrease in channel tortuosity, which reduces the flow resistance and improves the transport capacity of porous media.

Keywords: seepage, fractal Brownian motion, porous media, fractal dimension

PACS: 47.15.–x, 47.56.+r, 47.53.+n **DOI:** 10.1088/1674-1056/ab7b53

1. Introduction

Porous media are composite materials consisting of solid skeleton and pores with various sizes and shapes. Seepage phenomena in porous media are widely observed in nature and practical applications, such as water transport in soil,[1] oil and gas exploitation,[2] and drug delivery in vascular networks.[3] Existing studies have documented that the permeability characteristics of porous media depend on their pore structures and the physical properties of transported fluids.[4–6] However, since the pore distribution in most porous media is extremely intricate in reality, which includes interconnected and intricate channel network and pores with different sizes and shapes, it is still of great challenge to predict the seepage behavior accurately, and the quantitative relationship between structure parameters and permeability of porous media also needs to be further studied.

Scholars have carried out a lot of experimental[7,8] and theoretical[4,5,9] studies on the permeability characteristics of porous media for a long time. Most of the early research results are based on semi-empirical models, such as the Dacy model,[10] Brinkman–Forchheimer model,[11] and Kozeny–Carman model. Nevertheless, these models all contain empirical constants with no specific physical significance, which fails to characterize the seepage characteristics of porous media further. Moreover, due to the intricate internal channel network, the seepage behavior in porous media includes the intricate micro-boundary effect and the interaction between the solid matrix and fluid phase. Therefore, the available theoretical models can only predict the flow behavior in porous media with simple or regular structures. For irregular porous media, they are directly or indirectly regarded as a virtual continuum medium with uniform distribution on a large scale in practical applications. It is nearly impossible to describe the real pore structure of porous media accurately, but only to qualitatively demonstrate the internal flow behavior on a large scale rather than to reveal the micro-scale flow characteristics in porous media.

Due to the pioneering work of Mandelbrot,[12] the fractal theory has been widely applied in the investigations of heat and mass transfer in porous media in the last decades.[4,13,14] The introduction of fractal theory not only opens up a new way for the description of the irregular porous media but also makes it possible to reveal the percolation mechanism of porous media in depth. Pitchumani *et al.*[15] presented a fractal model of permeability without empirical constants during the research on percolation characteristics of porous fiber fabrics, which pioneered the introduction of fractal geometry to predict the flow behavior in porous media. Miao *et al.*[16] presented a fractal permeability model for the porous

*Project supported by the National Natural Science Foundation of China (Grant Nos. 51776037 and 51806147) and Natural Science Foundation of Jiangsu Province, China (Grant No. BK20170082).

†Corresponding author. E-mail: cbzhang@seu.edu.cn

© 2020 Chinese Physical Society and IOP Publishing Ltd

media, which is a function of the tortuosity fractal dimension, pore area fractal dimension, dimensionless pore size, and dimensionless pressure difference. Shen *et al.*[17] numerically studied the permeability in porous materials reconstructed by Sierpinski carpet based on a fractal model. Chen *et al.*[4] conducted a numerical study on seepage characteristics in fractal porous media constructed by Sierpinski carpet. The results indicated that the pore structure and connectivity plays a significant role in the permeability of porous media with identical porosity. However, most of the available fractal models for the construction of porous media are based on self-similar structure such as the Sierpinski carpet[4,17,18] and Menger sponge[19] (i.e., the fractal dimension is constant), which fails to demonstrate the randomness of pore structure in porous media. Kikkinides *et al.*[20] constructed a binary medium with both characteristics of randomness and statistical self-similarity based on the fractal Brownian motion (FBM). On this basis, a multi-dimensional fractal porous medium is developed by Türk *et al.*[21] via associating the stochastic function following the statistical characteristics of FBM with the properties of porous media. As a typical stochastic fractal model, FBM has proved its outstanding value in various practical applications, including terrain reconstruction,[22] pollutant diffusion,[23] and picture processing.[24] Kikkinides *et al.*[25] developed a binary medium generation method for generation of three-dimensional porous media based on the FBM model and validated its reliability by comparing the numerical predictions with the actual experiment for the permeability of the sandstone. Ma *et al.*[26] reconstructed the two-dimensional and three-dimensional porous media by the FBM model, and numerically investigated the gas diffusion characteristics in the porous media. Their results indicated that the numerical results of the effective diffusion coefficient agreed well with the experimental measurement. These previous research results have proved the practicability of the FBM method for construction of porous media with complex structures. Therefore, it is feasible to investigate the permeability characteristics of fractal porous media generated by the FBM method.

Based on a deep understanding of the FBM, a fractal model with an adjustable fractal dimension is developed to describe the solid matrix distribution of porous media quantitatively. With the reconstruction of fractal porous media, the mathematical model of single-phase fluid in fractal porous media is established and numerically studied with high priority to the role of solid matrix distribution in permeability characteristics. The flow characteristics in fractal porous media are compressively discussed and compared with those in homogeneous porous media, and the roles of fractal dimension and porosity in permeability characteristics of fractal porous media are quantitatively described.

2. Construction methodologies of porous media

The pore distribution and the solid matrix of most porous media are usually multi-scale, random, and statistically self-similar,[27–29] which is hard to describe by the traditional Euclidean geometry. Thanks to the pioneering work of Mandelbrot[12,29] and Kikkinides,[20] fractal geometry becomes an attractive application for characterizing porous media due to its intrinsic property of self-similarity. In their theory, the irregularity of pore distribution for porous media is quantitatively described by the fractal dimension.[20] Due to its outstanding merits in fractal description, the applications of the FBM model for porous media reconstruction are validated in the investigation of thermal conduction and mass transport.[30] Therefore, FBM is applied to reconstruct the solid matrix of porous media.

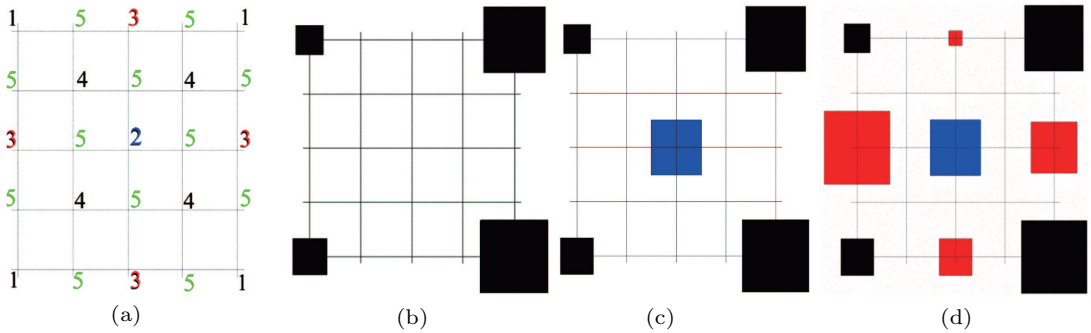


Fig. 1. Construction methodology of fractal porous media.

Due to its complex pore structure, the porous medium here is assumed to be two-dimensional, which is usually available in the literature.[4,20] A recursive method based on the random midpoint displacement algorithm is applied to describe the solid matrix distribution in the porous medium. A random function $f_{\mathrm{H}}(r)$ is defined as the methodology obeying FBM statistical properties. In this study, r represents the displacement and H is the Hurst exponent. In this methodology, the solid particle of porous media is regarded as a square, and its size is specified by $f_{\mathrm{H}}(r)$. Figure 1 shows the construction

methodology of the porous medium. As seen from the figure, a square zone is divided into sub-squares, with the number on the nodes (i.e., in Fig. 1(a)) representing the iteration number n. The generation scheme of fractal porous media is summarized as follows:

(1) Four solid particles are arranged at the corners of the square (see Fig. 1(b)), whose sizes are respectively acquired from the Gaussian distribution $N(0,\sigma_0^2)$.

(2) Then, the particle size at the square center shown in Fig. 1(c) is determined by the sum of the average of these at four corners and a random number F_1 generated from $N(0,\sigma_1^2)$. The size of the center solid particle is given by

$$f_{\mathrm{H},n}(r)=\frac{1}{4}\sum_{k=1}^{4}f_k(r)+F_1,\quad n=2, \tag{1}$$

where $f_k(r)$ represents the size of the solid particle denoted by 1. Here the increment variance of $f_{\mathrm{H},2}(r)$ is $2(\sigma_0^2/4+\sigma_1^2)$, and the displacement $r=1/\sqrt{2}$. Based on the scaling rule, we obtain

$$\sigma_1^2=\left(\frac{1}{\sqrt{2}}\right)^{2H}\sigma_0^2\left(1-2^{H-2}\right). \tag{2}$$

(3) Calculate $f_{\mathrm{H},3}(r)$ for the particle size at the edge midpoints (see Fig. 1(d)) by linear interpolation with adjacent corner values with F_2 obeying $N(0,\sigma_2^2)$. Thus, each particle size of the four edge midpoints is calculated by

$$f_{\mathrm{H},n}(r)=\frac{1}{2}\sum_{k=1}^{2}f_k(r)+F_2,\quad n=3. \tag{3}$$

According to the scaling rule of FBM, σ_2^2 can be related to σ_1^2 by the relationship given by

$$\sigma_2^2=\left(\frac{1}{\sqrt{2}}\right)^{2H}\sigma_1^2. \tag{4}$$

(4) Repeating the above steps (2) and (3) with a scaling factor $r=(1/\sqrt{2})^{2H}$ to describe the variance of space displacement, and the repetition is completed when the iteration number is $n=5$.

The statistical self-similarity of FBM depends on the Hurst exponent, which herein determines the spatial distribution of solid matrix for the fractal porous media as well. Moreover, the fractal dimension of the two-dimensional porous media relies on the Hurst exponent, $D=2-H$. For further understanding of the fractal dimension, Fig. 2 compares the pore structure of porous media with various fractal dimensions but identical porosity. The larger solid particles tend to be dispersive when the fractal dimension is larger (e.g., $D=1.8$). However, solid particles with different sizes separate more with a decrease in fractal dimension, where those of the same size tend to form a cluster, e.g., the case of $D=1.2$. This indicates that the fractal dimension affects the pore structure, and its increases will weaken the correlation of solid matrix and augment the pore connectivity in the fractal porous medium.

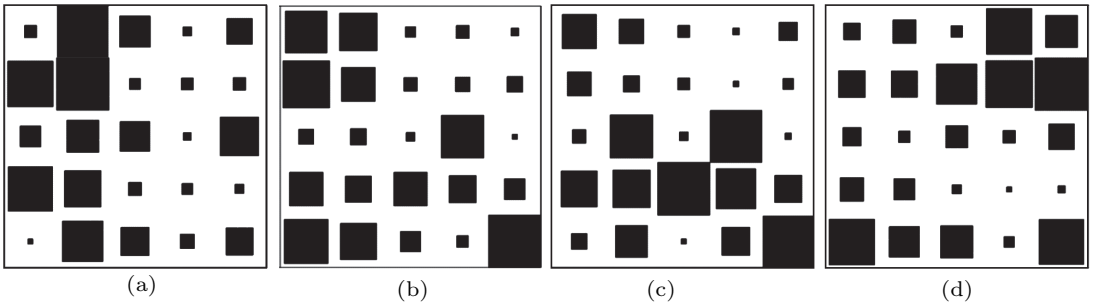


Fig. 2. The porous medium with various fractal dimension: (a) $D=1.2$, (b) $D=1.4$, (c) $D=1.6$, (d) $D=1.8$.

3. Seepage model and numerical solution

3.1. Physical model

Due to the merits of randomness and the statistical self-similarity of FBM, the solid matrix of the two-dimensional fractal porous medium is reconstructed herein. Water is used as a working medium, and its physical properties are listed in Table 1. To study the seepage characteristics of porous media, the schematic of laminar flow in fractal porous media is shown in Fig. 3. As demonstrated in the figure, the test channel has a length $L=30$ mm and an inner width $W=5$ mm. The middle part is a two-dimensional fractal porous medium with a dimension of $L_0\times L_0=5$ mm $\times 5$ mm. Among them, the white part is the interconnected pores, and the black part is the solid matrix. The lengths of entrance and exit are identical, i.e., $L_{\mathrm{in}}=L_{\mathrm{out}}=12.5$ mm. The volume flow rate $Q=10$ mL/s is initially imposed at the inlet of the straight channel.

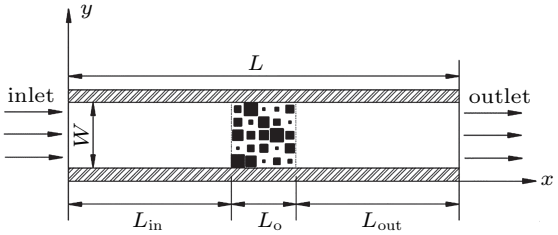


Fig. 3. Schematic diagram of laminar flow in the fractal porous medium.

Table 1. Physical parameters of water.

Physical property	Water
Temperature/℃	20
Density/(kg/m^3)	998.2
Viscosity/(kg/m·s)	0.001003

3.2. Governing equations

For simplification of the numerical solution, serial assumptions should be made in this paper: (1) Steady laminar flow. (2) The liquid–solid interface is the no-slip boundary. (3) The physical parameters of the fluid are constant. (4) The mass force item is ignorable.

It has been documented that the liquid flow in porous media such as oil and gas exploitation, groundwater infiltration, and blood flow in the vascular network can be assumed to be laminar flow, in which the Reynolds number of internal flow is small.[31] Based on these assumptions, the governing equations for laminar flow in our porous medium can be given by the continuity equation

$$\frac{\partial u}{\partial x}+\frac{\partial v}{\partial y}=0, \tag{5}$$

and the momentum equations

$$u\frac{\partial u}{\partial x}+v\frac{\partial u}{\partial y}=-\frac{1}{\rho}\frac{\partial p}{\partial x}+\upsilon\left(\frac{\partial^2 u}{\partial x^2}+\frac{\partial^2 u}{\partial y^2}\right), \tag{6}$$

$$u\frac{\partial v}{\partial x}+v\frac{\partial v}{\partial y}=-\frac{1}{\rho}\frac{\partial p}{\partial y}+\upsilon\left(\frac{\partial^2 v}{\partial x^2}+\frac{\partial^2 v}{\partial y^2}\right), \tag{7}$$

where u and v represent the velocity of water, p represents the pressure, ρ represents the density, and υ is the kinematic viscosity of water.

3.3. Boundary conditions

The volume flow rate at the inlet of the channel is regarded as constant. Therefore, the constant velocity condition is set to be the inlet boundary condition, which can be written as

$$x=0,\quad u=u_{\text{inlet}},\quad v=0. \tag{8}$$

In addition, the fluid at the outlet of the straight channel is assumed to be a fully developed flow, like most engineering applications. Therefore, the outlet boundary condition is given by

$$x=L,\quad \frac{\partial u}{\partial x}=\frac{\partial v}{\partial x}=0. \tag{9}$$

The solid-liquid interfaces are assumed to be no-slip boundaries, that is, the fractional velocities u and v in the x and y directions at solid-liquid interfaces satisfy the following relationship

$$u=v=0. \tag{10}$$

3.4. Numerical approach and grid checking

In the present work, the commercial CFD software Fluent is used to study the seepage characteristics of the two-dimensional porous medium. To acquire the velocity and pressure distribution of fluid in the porous medium, the governing equations are solved by the finite volume method with a dual-precision solver. The momentum equation and pressure term are discretized by the second-order upwind scheme, and the convection term is discretized by the fully implicit mixed difference scheme. Moreover, the SIMPLE algorithm is utilized to determine the pressure-velocity coupling. A series of discrete equations in terms of velocity and pressure can be obtained by integrating the discretized equations in each control volume. For better convergence accuracy of the calculation, the Gauss–Seidel method considering the over-relaxation factor is applied to solve all the discrete equations. The iteration is regarded to be convergent when the maximum residuals of velocity and pressure after iteration are both less than 10^{-6}. Furthermore, the iterative calculation can also be considered to be converged when the average velocity at the channel outlet remains constant.

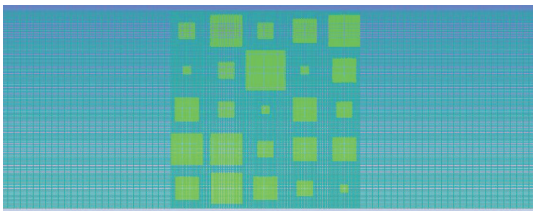


Fig. 4. Grid schematic of the computational domain.

To perform the numerical solution based on the present model, a structured grid system is used to divide the computational domain, as shown in Fig. 4. The liquid and solid phases in the channel are divided into quadrilateral elements. Moreover, local mesh refinement is conducted for the region of the porous medium to improve the accuracy of the calculation. In addition, the grid independence test is carried out for various numbers of nodes to ensure that the numerical results are independent of the grid system. The velocity distributions of the porous medium with porosity $\varepsilon=0.7$ under different grid systems are depicted in Fig. 5. It is evident that with the increase in the number of nodes, the local velocity difference of the porous medium becomes more obvious. However, when the number of nodes is larger than 170821, the velocity distribution in the porous medium tends to be identical. Simultaneously, the average velocity at the channel outlet illustrated in Fig. 6 remains constant as well. In this study, considering the saving of computing resources and time consumption, we choose a grid system with the number of nodes $N_{\text{n}}=170821$ for calculation.

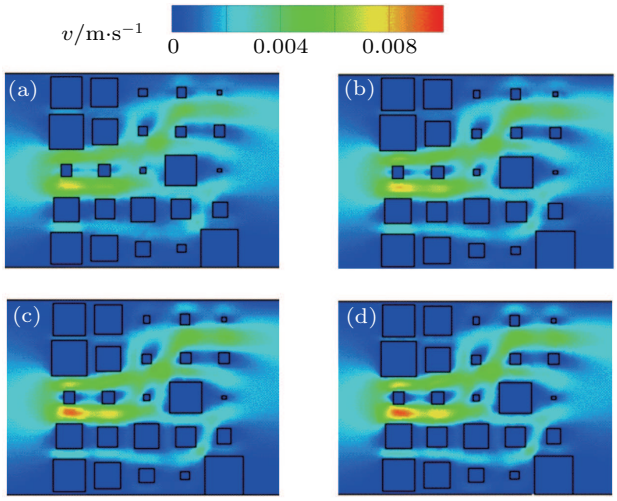


Fig. 5. Effect of number of nodes on velocity distribution in the porous medium ($\varepsilon = 0.7$): (a) $N_n = 62425$, (b) $N_n = 125446$, (c) $N_n = 170821$, (d) $N_n = 188964$.

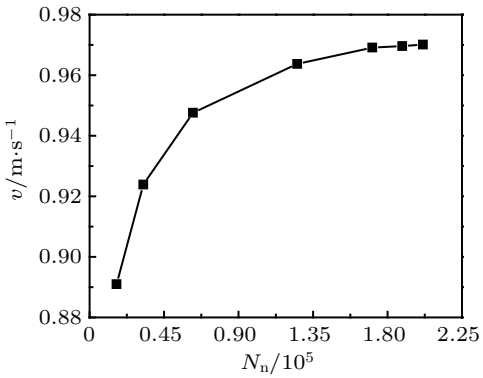


Fig. 6. Effect of number of nodes on velocity at channel outlet ($\varepsilon = 0.7$).

3.5. Model validation

To verify the present model, a numerical investigation on the liquid flow in the two-dimensional porous medium with different porosities is conducted here. The numerical results from the current model are compared with those of the Kozeny–Carman equation[32]

$$k = \frac{c_0}{M^2}\frac{\varepsilon^3}{(1-\varepsilon)^2}, \tag{11}$$

where ε is the porosity of the porous medium, M is the area of specific surface, k is permeability, c_0 is Kozeny's constant, which depends on the geometrical cross-section of the tubes.

A comparison between the numerical predictions and the Kozeny–Carman results for the dimensionless permeability in the two-dimensional porous medium is given in Fig. 7. As is shown, there is a small discrepancy between the numerical and Kozeny–Carman results. The explanation is that the Kozeny–Carman results are achieved based on the assumption that the channels in the porous medium are straight tubes, which is different from the present model. Still, the numerical results from the current model agree with the Kozeny–Carman results. Consequently, it can be considered that the current model is reasonable and can predict the seepage characteristics in the fractal porous medium.

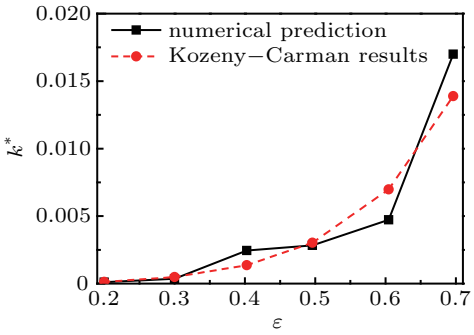


Fig. 7. Comparison of the numerical predictions and the Kozeny–Carman results.

4. Results and discussion

4.1. Seepage behavior analysis

The randomness of the pore structure makes the channel network in the porous medium very complex. Fluid flows in interconnected pores are distorted, which has a significant impact on the permeability characteristics of the porous medium. To reveal the percolation mechanism in the porous medium, Fig. 8 illustrates the velocity and vector distribution in the fractal and homogeneous porous medium. It is seen that along the flow direction, the fluid is more inclined to converge at the large aperture channel so the velocity in the large aperture channel is also larger, and the peak velocity appears in its throat. However, the velocity of water in the narrow channel is smaller, and that in the wake area of some large solid particle is nearly zero. Moreover, due to the non-uniform distribution of the solid matrix, the internal channels in the fractal porous medium are tortuous and vary in aperture, so that the velocity in the fractal porous medium is not uniform. On the contrary, the flow channel inside the homogeneous porous medium is relatively straight, and the aperture difference is not significant, so the velocity field inside the homogeneous porous medium is relatively homogeneous.

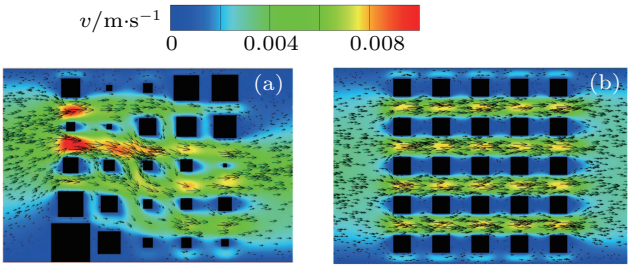


Fig. 8. Velocity and vector distribution in the fractal and homogeneous porous medium ($\varepsilon = 0.8$): (a) fractal porous medium, (b) homogeneous porous medium.

To further understand the effect of solid matrix distribution on the flow characteristics, the pressure distribution and streamline diagrams in the fractal and homogeneous porous

medium are demonstrated in Fig. 9. The streamline in the homogeneous porous medium is nearly straight. Due to the obstruction of solid matrix distributed in inhomogeneous fashion, the streamline in the fractal porous medium is no longer a straight line but a tortuous curve. Moreover, the pressure distribution in the fractal porous medium is non-uniform compared to that in the homogeneous porous medium. However, although the channel tortuosity in the fractal porous medium is larger, the pressure drop along the path is smaller than that in the homogeneous porous medium. The explanation is that random distribution of solid matrix in the fractal porous medium may provide some larger aperture channels for the fluid flow, reducing the overall pressure drop loss along the way. Therefore, it is of great significance to study the role of pore structure in the percolation characteristics of the porous medium.

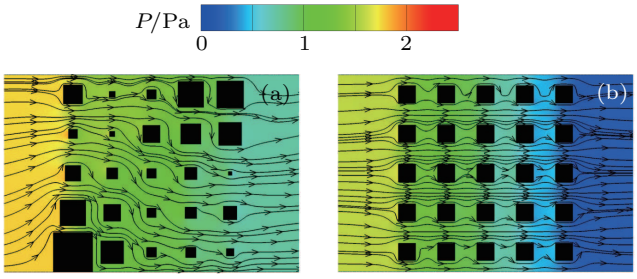


Fig. 9. Pressure distribution and streamline diagrams in the fractal and homogeneous porous medium ($\varepsilon = 0.8$): (a) fractal porous medium, (b) homogeneous porous medium.

4.2. Reynolds number criterion

It has been documented that when the Reynolds number is low, the liquid flow in the porous medium agrees well with the Darcy law.[33] In general, the permeability is utilized to characterize the percolation behavior in the porous medium. However, it usually depends on the dimension of the porous medium, which fails to reveal the inherent characteristics of percolation. Therefore, the dimensionless permeability is introduced to describe the transport capacity of the porous medium. The dimensionless parameter is calculated by

$$k^* = \frac{k}{d_e^2} = \frac{Q\mu L_o}{A\Delta p d_e^2}, \tag{12}$$

where k is permeability, A the cross-sectional area of the pore domain, Δp denotes the pressure difference between two ends of the porous medium, μ represents the dynamic viscosity of water, and d_e the effective hydraulic diameter of the inner channels in the porous medium, which is defined as the ratio of the volume of the channels to its wetted surface area. The expression is given by

$$d_e = \frac{2\varepsilon}{M}, \tag{13}$$

where ε represents the porosity of the porous medium, and M is the specific surface of the porous medium.

Previous studies have shown that Darcy's law can only be applied when the percolation rate is small.[33] With the increase of percolation rate, the flow characteristics in the porous medium will gradually deviate from Darcy's law. To determine the range of percolation rate in which flow characteristics satisfy the Darcy law, the seepage behaviors in the porous medium are analogized to these in tubes. Here the Reynolds number can be written as

$$Re = \frac{v d_e}{\bar{v}}, \tag{14}$$

where Re is the Reynolds number, $\bar{v}$ is the percolation rate of the porous medium, and $\bar{v} = Q/(\varepsilon \times A)$. Moreover, the friction drag coefficient along the path can be calculated by

$$\lambda = \frac{2\Delta p d_e}{\rho \bar{v}^2 L_0}, \tag{15}$$

where λ is the friction drag coefficient of the porous medium.

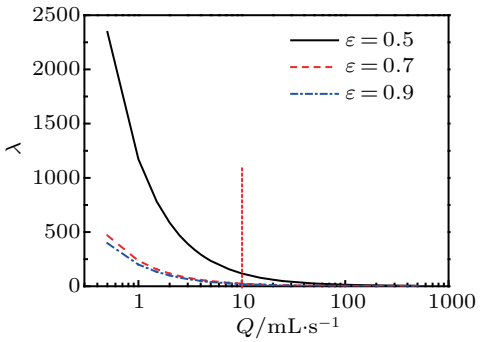


Fig. 10. Effect of volume flow rate on friction drag coefficient ($D = 1.8$).

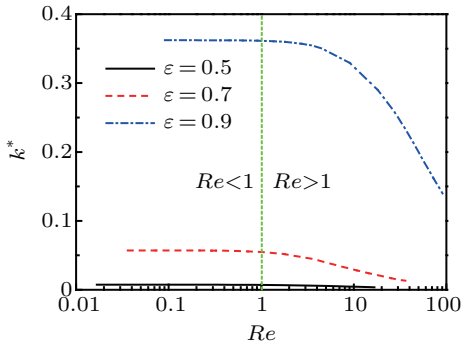


Fig. 11. Effect of Reynolds number on dimensionless permeability ($D = 1.8$).

The relationship between the volume flow rate and the friction drag coefficient is illustrated in Fig. 10. The porosity is negatively correlated to the friction drag coefficient through the porous medium. Moreover, the volume flow rate through the porous medium is inversely proportional to the friction drag coefficient when it is less than 10 mL/s. However, with the further increase in the inlet volume flow rate, the evolution tendency gradually deviates from the inversely-proportional relationship, and the larger the porosity, the greater the deviation. It attributes that the liquid flow in the porous medium is a coupling effect of inertial and viscous forces when the volume flow rate is large. To further determine the Reynolds

number criterion, the variation of dimensionless permeability of the porous medium with Reynolds number is depicted in Fig. 11. As is expected, there is a transition point in the effect of Reynolds number on dimensionless permeability of the porous medium. When the Reynolds number $Re < 1$, the dimensionless permeability is almost independent of the Reynolds number, but further increase in the Reynolds number leads to a smaller permeability. This is, Darcy's law cannot accurately describe the seepage characteristics of the porous medium when $Re > 1$.

4.3. Structural parameters analysis

4.3.1. Effect of porosity

As one of the important structural parameters, porosity visually presents the pore occupancy of the porous medium, which plays a significant role in the seepage performance of the porous medium. On account that the pores of the porous medium considered in the current work are interconnected, the increase of porosity contributes to higher connectivity and enlarged equivalent diameter of the internal channel network, enhancing the permeability of the fractal porous medium. To study the role of porosity in the permeability of the fractal porous medium, Fig. 12 depicts the variation of dimensionless permeability with porosity. The entrance flow rate of all cases here is 10 mL/s. As is expected, the dimensionless permeability of the fractal porous medium increases monotonously with the augment of porosity. It is interesting that when $\varepsilon < 0.6$, the dimensionless permeability of the fractal porous medium is small, and its variation with porosity is small as well. However, with the further augment of porosity, there is a rapid increase in the dimensionless permeability of the fractal porous medium.

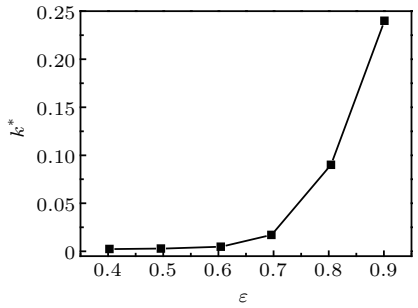


Fig. 12. Effect of porosity on dimensionless permeability ($D = 1.2$).

Figure 13 further demonstrates the flow characteristics in the porous medium with different porosities. It is evident that with the increase of porosity, the equivalent diameter of the internal channel network is enlarged, and the peak velocity of the fluid decreases gradually, which leads to a more uniform development in velocity distribution so that the effective seepage performance of the porous medium is enhanced. As shown in the figure, most fluid flows through the lower part of the porous medium when its porosity is 0.5, which results in a polarization trend in velocity distribution. For the case of $\varepsilon = 0.8$, the velocity distribution of the porous medium is more uniform due to the increase of equivalent aperture and the decrease of channel aperture difference. Furthermore, it is clear that with the augment of porosity, the pressure drop through the porous medium decreases gradually due to the decrease of the tortuosity of streamline, and the permeability of the porous medium is augmented accordingly. It is noteworthy that the pressure loss through the porous medium is larger when porosity is less than 0.6, which seriously weakens the permeability of the porous medium. Nevertheless, when $\varepsilon > 0.6$, the pressure loss through the porous medium is very small, and the seepage performance of the porous medium is enhanced.

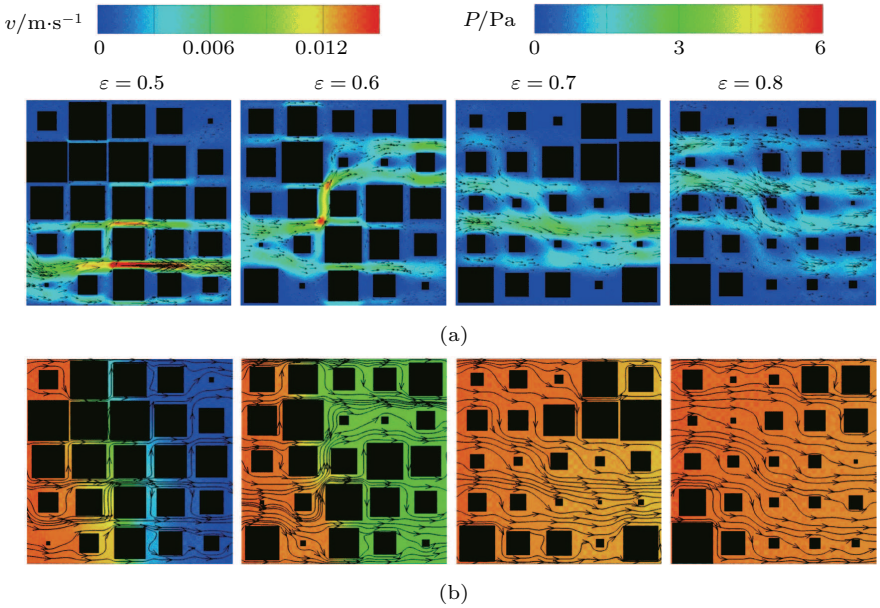


Fig. 13. Effect of porosity on flow characteristics in the porous medium ($D = 1.2$): (a) velocity and vector distribution, (b) pressure distribution and streamline diagram.

4.3.2. Effect of fractal dimension

The fractal dimension of the porous medium constructed by the FBM model is applied to characterize the structural correlation of pores or solid matrix in the porous medium to some extent.[20,21] The pore structure in the fractal porous medium varies with the fractal dimension. Consequently, the fractal dimension significantly affects the seepage characteristics of the fractal porous medium as well though the porosity is identical. The dimensionless permeability of the fractal porous medium with different fractal dimensions is illustrated in Fig. 14 under the condition with an inlet volume flow rate of 10 mL/s. The figure indicates that the fractal dimension is positively correlated with the dimensionless permeability of the porous medium. With the augment in the fractal dimension, the dimensionless permeability increases nonlinearly as well. This is on account that with the augment of fractal dimension, the structural correlation of solid matrix in the porous medium decreases, which augments the connectivity of the internal channel network in the porous medium, enhancing the transport capacity of the porous medium.

For further insight into the role of fractal dimension in the seepage characteristics of the porous medium, Fig. 15 shows the permeability characteristics in the porous medium with various fractal dimensions. It is seen that with the augment of fractal dimension, the maximum equivalent aperture in the porous medium increases gradually. Nevertheless, although the peak velocity in the porous medium decreases, the overall percolation rate of the porous medium increases gradually. Furthermore, the fractal dimension is negatively correlated with the pressure drop through the porous medium. This is, the pressure loss through the fractal porous medium decreases gradually with the augment of fractal dimension. The explanation is that the correlation of solid matrix decreases with the decrease of fractal dimension, the streamline tends to be straight and the tortuosity decreases, which reduces the pressure drop through the porous medium and enhances the transport capacity of the porous medium. Therefore, a porous medium with a higher fractal dimension is expected to enjoy a better seepage performance.

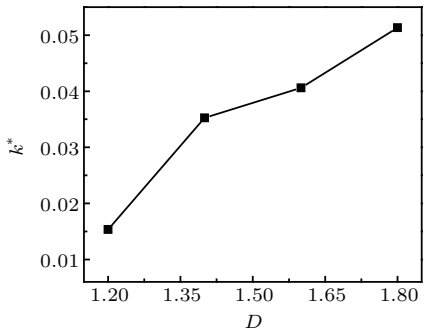


Fig. 14. Effect of fractal dimension on dimensionless permeability ($\varepsilon = 0.7$).

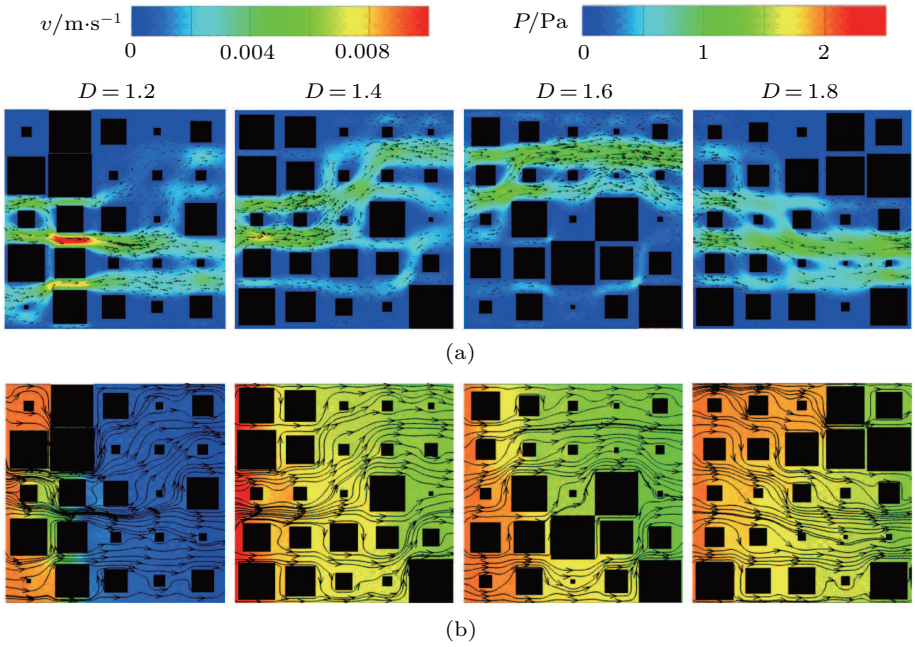


Fig. 15. Effect of fractal dimension on flow characteristics in the porous medium ($\varepsilon = 0.7$): (a) velocity and vector distribution, (b) pressure distribution and streamline diagram.

5. Conclusion

The fractal Brownian motion (FBM) model is utilized to quantitatively describe and reconstruct the porous structure of a porous medium in the present work. The numerical model of liquid flow in the porous medium is developed and solved with emphasis on the role of solid matrix distribution. The flow characteristics in the fractal porous medium are analyzed and compared with those in the homogeneous one, and the roles of the fractal dimension and porosity in the seepage characteristics of the porous medium are given as well. The conclusions

are summarized as follows:

(1) The pressure and velocity distributions in the fractal porous medium are non-uniform due to the tortuous internal channels and different aperture sizes. The streamline in the fractal porous medium is no longer a straight line but a tortuous curve. Along the flow direction, the velocity in the large aperture channel is larger, and the peak velocity appears in its throat, while the velocity in the narrow channel is small, and the velocities in the wake region of some large solid particles are nearly zero.

(2) There is a transition point in the influence of Reynolds number on dimensionless permeability of the porous medium. When $Re < 1$, the dimensionless permeability of the fractal porous medium remains constant. However, with the further increase of Reynolds number, the dimensionless permeability decreases gradually, which indicates that it is impossible to use Darcy's law to accurately predict the seepage behavior in the porous medium when $Re > 1$.

(3) Porosity is an important factor affecting the seepage characteristics of the porous medium. The permeability of the fractal porous medium increases monotonously with the increase of porosity due to the higher connectivity and enlarged equivalent aperture of the internal channel network. It is interesting that the dimensionless permeability only has a slight variation when $\varepsilon < 0.6$, while a further increase in porosity leads to a rapid augment in the dimensionless permeability of the porous medium.

(4) Though the porosity is identical, the fractal dimension also plays a significant role in the seepage characteristics of the porous medium. The structural correlation of the solid matrix in the porous medium decreases with the augment in the fractal dimension. In this study, the connectivity of channel network in the porous medium is enhanced, and the channel tortuosity is decreased, which reduces the flow resistance loss and augments the transport capacity of the porous medium.

References

[1] Ding H R, Liu J X, Cui Z W and Kundu T 2017 *Chin. Phys. B* **26** 124301
[2] Xu P, Li C H, Qiu S X and Sasmito A P 2016 *Fractals.* **24** 1650018
[3] Chen Y P, Gao W, Zhang C B and Zhao Y J 2016 *Lab Chip* **16** 1332
[4] Chen Y P, Shen C Q, Lu P F and Huang Y P 2015 *Chem. Eng. Process.* **87** 75
[5] Zou H, Deng S C and Li H B 2019 *Chin. Phys. B* **28** 030202
[6] Hansen A, Sinha S, Bedeaux D, Kjelstrup S, Gjennestad M A and Vassvik M 2018 *Transport. Porous. Med.* **125** 565
[7] Li B, Zhang Z W, He Z B et al 2015 *High Power Laser Part. Beams* **27** 032024 (in Chinese)
[8] Wang T, Zheng K C, Jia Y P, Fu C L, Gong Z J and Wu W F 2017 *Chin. Phys. B* **26** 074701
[9] Chen Y P, Liu X D and Shi M H 2013 *Appl. Phys. Lett.* **102** 051609
[10] Whitaker S 1986 *Transport. Porous. Med.* **1** 3
[11] Bhatti M M, Zeeshan A, Ellahi R and Shit G C 2018 *Adv. Powder Technol.* **29** 1189
[12] Mandelbort B B, Passoja D E and Paullay A J 1984 *Nature* **308** 721
[13] Chen Y P and Deng Z L 2017 *J. Fluid Mech.* **819** 401
[14] Huo Y T, Guo Y Q and Rao Z H 2019 *Int. J. Energ. Res.* **43** 767
[15] Pitchumani R and Yao S C 1991 *J. Heat Transfer.* **113** 788
[16] Miao T J, Chen A M, Xu Y, Cheng S J and Yu B M 2019 *Fractals* **27** 1950121
[17] Shen X W, Cui W Z and Feng Y 2018 *Int. J. Heat Mass Transf.* **121** 1307
[18] Reis F D A A 2019 *Adv. Water Res.* **134** 103428
[19] Yang Y, Feng Y T and Yu Y H 2017 *Fractals.* **25** 1750040
[20] Kikkinides E S and Burganos V N 1999 *Phys. Rev. E* **59** 7185
[21] Türk C, Carbone A and Chiaia B M 2010 *Phys. Rev. E* **81** 026706
[22] Lv C Y and Yu F 2018 *Math. Probl. Eng.* **2018** 8641471
[23] Qin R F, Lin L Z, Kuang C P, Su T C, Mao X M and Zhou Y S 2017 *Environ. Model. Softw.* **92** 252
[24] Kumar M, Kumar S, Das M K, Budhiraja R and Singh S 2018 *J. Inf. Secur. Appl.* **40** 134
[25] Kikkinides E S and Burganous V N 2000 *Phys. Rev. Lett.* **62** 6906
[26] Ma Q and Chen Z Q 2014 *Int. J. Heat Mass Transf.* **79** 925
[27] Rubio M A, Edwards C A, Dougherty A and Gollub J P 1989 *Phys. Rev. Lett.* **63** 1685
[28] Timothy J J and Meschke G 2018 *Transport. Porous. Med.* **125** 413
[29] Mandelbrot B B 1985 *Phys. Scripta.* **32** 257
[30] Xu W, Liang Y J, Chen W and Cushman J H 2019 *Int. J. Heat Mass Transf.* **139** 39
[31] Liu S J, Afacan A and Masliyah J 1994 *Chem. Eng. Sci.* **49** 3565
[32] Schulz R, Ray N, Zech S, Rupp A and Knabner P 2019 *Transport. Porous. Med.* **130** 487
[33] Koponen A, Kataja M and Tomonen J 1997 *Phys. Rev. E* **56** 3319